Design of Resonator-Coupled Wireless Power Transfer System by Use of BPF Theory

Ikuo Awai · Tetsuya Ishida

Abstract

A wireless power transfer system based on magnetically coupled two resonators is analysed using the filter theory. Design equations for each lumped parameter circuit components are derived. As a result, change of coupling coefficient between the resonators and/or change of load resistance are easily responded. Effect of circuit loss to the design theory is also addressed. After designing a power transfer system, a real system is constructed using spiral and loop coils. Dependence of circuit elements on their dimensions is measured in advance and used to cope with the designed element values. Simulated response by use of designed element values and measured result are compared, indicating the validity of the theory.

Key words : BPF Design Theory, Magnetically Coupled Resonators, Simulation and Experiment, System Design, Wireless Power Transfer.

Ⅰ. Introduction

After MIT group has proposed a resonator-coupled wireless power transfer (WPT) system [1], many people in the world have tried to confirm and/or improve the transfer property of the similar system. But partly because their theory is based on the intricate coupled mode theory and, in addition, all the necessary information does not seem to be disclosed, there is no design theory presented so far to our knowledge.

Considering that they use two coupled resonators facing each other and try to match them with the external circuits, their system is neither more nor less that a 2-stage band pass filter. Since the design theory of a BPF is well established [2], its modification is expected to give a simple and clear design theory of the wireless power transfer system [3, 4].

Since the BPF design is built for LCR circuits, our theory gives the relation of each circuit element. Thus, one has to find the equivalent circuit of the system first, and then the dependence of each element value on their dimensions beforehand. Using the designed element value and the dependence above, one can determine the structure of the system.

We will take the MIT system as an example. But the theory can be applied for any magnetically coupled resonator system, and could be extended to electrically coupled systems easily. Some design examples will be shown together with the simulated response and the experimental results. Their reasonable agreement verifies the effectiveness of the design theory.

Ⅱ. Equivalent Circuit

The rough sketch of MIT system is depicted in Fig. 1. The coupling between the loop and spiral coils and also between two spiral coils is substantially magnetic, and thus, the coupling circuit should be expressed by mutual inductance circuit. In Fig. 2, an equivalent circuit of the power transfer system in Fig. 1 is described, where L_g denotes the self inductance of input loop coil, M_g the mutual inductance between the input loop coil and adjacent spiral coil, L_0 the self inductance of the spiral coil, C_0 the stray capacitance between wires of spiral coil, C_e the stray capacitance between spiral coil and the ground.

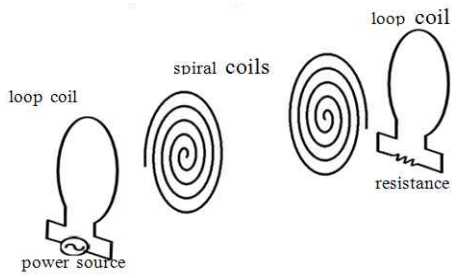

Fig. 1. Wireless power transfer system based on magnetically coupled two resonators.

Manuscript received October 1, 2010 ; revised December 6, 2010. (ID No. 20101001-08J)
Department of Electronics & Informatics, Ryukoku University, Otsu, Japan.
Corresponding Author : Ikuo Awai (e-mail : awai@rins.ryukoku.ac.jp)

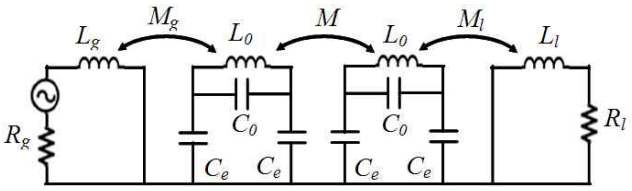

Fig. 2. Equivalent circuit of Fig. 1.

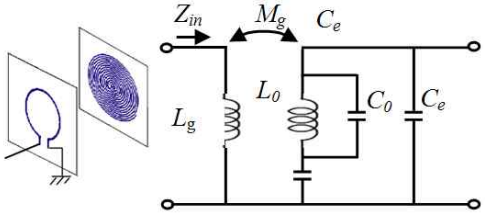

Fig. 3. Equivalent circuit of a loop coil coupled to a spiral coil.

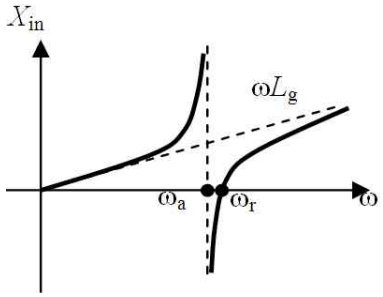

Fig. 4. Frequency characteristic of input reactance of circuit in Fig. 3.

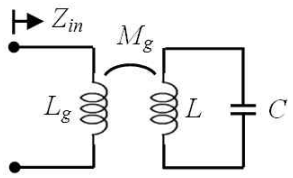

Fig. 5. Simplified equivalent circuit of a loop coil coupled to a spiral coil and its input impedance.

Considering the spiral coils are not directly connected to the circuit, the value of C_e could be quite unstable, depending on the objects around it and their arrangement. But in reality, the fluctuation is not so serious in its value that we can rely on the reproducibility of the system response. It is needless to say that we should not put any obstacles close to the system.

We calculate the input impedance of the loop coil coupled to a spiral coil as shown in the inset of Fig. 3. The input reactance is obtained to show the series and parallel resonances by ω_r and ω_a as depicted in Fig. 4, respectively.

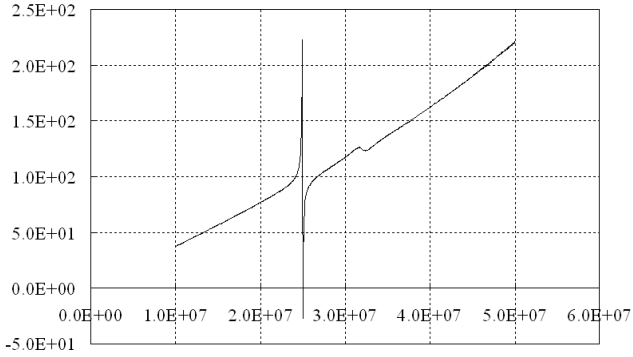

Fig. 6. Typical frequency characteristic of input reactance of loop coil coupled to spiral coil (measured result).

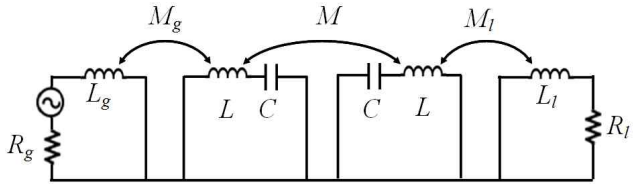

Fig. 7. Equivalent circuit of power transfer system.

Considering that the capacitors connecting to the inductor L_0 in Fig. 3 could be reduced to one capacitor, we calculate the input impedance of the circuit in Fig. 5. It turned out to show the similar frequency characteristics as that shown in Fig. 4. To confirm the process above, we have measured a typical loop coil coupled to a spiral coil that has the configuration shown in Fig. 3. The measured frequency characteristic in Fig. 6 shows the same behaviour as Fig. 4, and hence, the simplified circuit in Fig. 5 is safely adopted for the equivalent circuit representation of the system in Fig 1. We will utilize Fig. 7 as the equivalent circuit to design the WPT system shown in Fig. 1.

Ⅲ. Circuit Transform

The mutual inductance circuit in Fig. 8(a) is equivalent to the circuit in (b). Therefore, the circuit in Fig. 7 is transformed into Fig. 9.

On the other hand, the T circuit shown in Fig. 10(a) constitutes a K inverter with the characteristic impedance ω_rM as shown in (b). Thus, the circuit in Fig. 9 is finally converted into Fig. 11. The conversion to

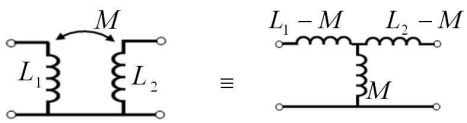

Fig. 8. Equivalence of mutual inductance circuit to T circuit.

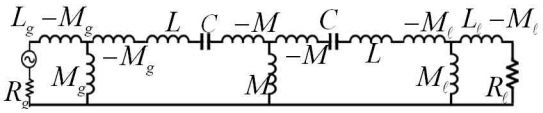

Fig. 9. First transformation of original circuit.

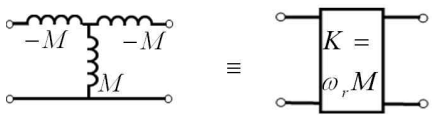

Fig. 10. Realization of K inverter.

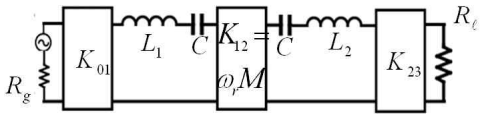

Fig. 11. Final transformation of power transfer circuit.

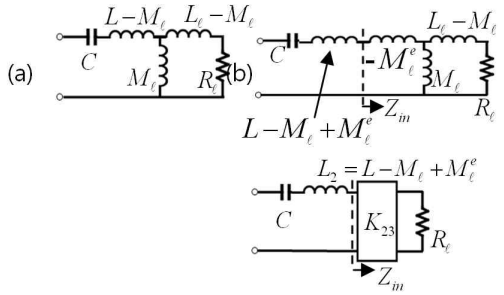

Fig. 12. Transformation of circuit including inductance and resistance.

the inverter K_{12} is straightforward, but that to K_{01} and K_{23} needs some manipulation, since we have to delete the self inductance L_g and L_l. The inductances L_1 and L_2 will be given later.

Take the conversion of the load resistance side of Fig. 9 as an example.

Fig. 12 shows the process of conversion. One adds a negative inductance $-M_\ell^e$ to the circuit in (a) and subtract it from the series inductance $L - M_l$ as shown in (b). Then, the input impedance Z_{in} is calculated as

$$Z_{in} = -j\omega_r M_\ell^e + \frac{1}{\frac{1}{j\omega_r M_\ell} + \frac{1}{j\omega_r (L_\ell - M_\ell) + R_\ell}} \tag{1}$$

The input impedance in (b) is equated to that in (c) which is

$$Z_{in} = \frac{K_{23}^2}{R_\ell} \tag{2}$$

Comparison of the real and imaginary part of eqs. (1) and (2) gives

$$K_{23} = \frac{\omega_r M_l R_\ell}{\sqrt{R_l^2 + (\omega_r L_l)^2}}$$
$$M_\ell^e = M_\ell - \frac{\omega_r^2 M_\ell^2 L_\ell}{R_\ell^2 + (\omega_r L_\ell)^2} \tag{3}$$

It means that introduction of negative inductance has cancelled the cumbersome inductance L_l. As a result, the inductance $L - M_l$ is changed into

$$L_2 = L - M_\ell + M_\ell^e \tag{4}$$

The same procedure is applied to the generator side, and one obtains

$$K_{01} = \frac{\omega_r M_g R_g}{\sqrt{R_g^2 + (\omega_r L_g)^2}},$$
$$M_g^e = M_g - \frac{\omega_r^2 M_g^2 L_g}{R_g^2 + (\omega_r L_g)^2} \tag{5}$$

and

$$L_1 = L - M_g + M_g^e \tag{6}$$

$$K_{12} = \omega_r M \tag{7}$$

Ⅳ. Condition for 2-Stage BPF

The circuit shown in Fig. 11 is one of the standard circuits for BPF design. The first condition for a matched BPF claims the resonant frequency of each resonator is the same, that is,

$$L_1 C = L_2 C = 1/\omega_r^2 \tag{8}$$

Though the equation above insists that L_1 and L_2 are equal each other, we have remained the possibility of unequalness so far.

In the second, the characteristic impedance of each inverter should satisfy the conditions

$$K_{01} = \sqrt{\frac{w\omega_r R_g L_1}{g_0 g_1}}, K_{12} = \omega_r w \sqrt{\frac{L_1 L_2}{g_1 g_2}}, K_{23} = \sqrt{\frac{w\omega_r R_l L_2}{g_2 g_3}} \tag{9}$$

where g_0 to g_3 are g-values of the prototype low pass filter, ω_r is the center angular frequency of the BPF, and w is the fractional bandwidth, that is, the bandwidth divided by the center frequency. The g-values are automatically decided when one takes Butterworth type filter, for example.

Now, let us consider how the design of power transfer system is carried out. First, the input resistance of the generator R_g is given. The key component of system is probably the spiral coil, since it determines the outreach of power transfer as well as the transfer efficiency.

Then the parameters L and C are determined first (since there is no need to have different values for two spiral coils, they are assumed the same). The mutual inductance M (or coupling coefficient k) is affected by the distance between coils, and hence, is suspended to decide.

The loop coils are used to attain the circuit matching. They can be slid to change the coupling to the helical coil. In that usage, the self inductance L_g and L_l will be given because one has to prepare the coils first. In summary, we give the parameter L, C, and R_g first, and then, L_g and L_l. The tuneable parameters should be the mutual inductance of helical coils M, the load resistance R_l, and the mutual inductances M_g and M_l.

Referring to all the equations from eq. (1) to eq. (9), one obtains the very simple relations as follows,

$$M_g = \sqrt{(1+Q_{eg}^2)\frac{R_g}{\omega_r}M} \tag{10}$$

$$\frac{M_\ell}{M_g} = \sqrt{\frac{R_\ell}{R_g}} \tag{11}$$

$$\frac{L_\ell}{L_g} = \frac{R_\ell}{R_g} \tag{12}$$

$$C' = \frac{C}{1-\dfrac{Q_{eg}^2 k_g^2}{1+Q_{eg}^2}} \tag{13}$$

where k_g is the coupling coefficient between the loop and helical coils at the generator side, and Q_{eg} is the external Q of the loop coil at the generator side, too.

$$k_g = \frac{M_g}{\sqrt{L_g L}} \tag{14}$$

$$Q_{eg} = \frac{\omega_r L_g}{R_g} \tag{15}$$

Equation (13) indicates that the capacitance C of the helical coil should be adjusted in order to keep the center frequency of the BPF as designed at the beginning. It happened because the helical coil is influenced by the loop coil coupled with the external circuit.

When the coupling between two helical coils changes, M_g should be adjusted according to eq. (10) together with M_l, being related with M_g as shown in eq. (11). But the self inductance of loop coil is allowed to be constant. It means that the change of distance between two helical coils is responded only by adjusting the distance between the helical and loop coils.

If the load resistance R_l changes, both the self inductance and mutual inductance of the load loop coil should be adjusted due to eqs. (11) and (12). In order for the self inductance to be changed, the coil itself should be deformed. But for the mutual inductance, only the distance to the helical coil can be adjusted. There is no influence to the two helical coils.

These characteristics above have never presented though each one can be half expected. The clearly-stated relations, eqs. (10) to (15) will help design the magnetically coupled power transfer system.

Ⅴ. Dependence of Circuit Elements on Their Dimensions

In order to construct a WPT system, one needs to prepare the parametric dependence of each circuit element. It could be obtained either by E/M simulation or experiment. We will take experiment, since the simulation of coils takes too much cpu time.

In construction of the system, one should determine what kind of resonators are chosen. We will take spiral resonators with a certain pitch. Then, the operating frequency is to be decided, which gives the inductance L and the effective capacitance C in Fig. 7. The inductance of the fabricated spiral coil is measured with an LC meter at a low frequency, e. g. 100 kHz, and the capacitance is calculated by the relation

$$LC = \frac{1}{\omega_r^2} \tag{16}$$

since it can not be measured.

Next, we have to decide the distance between two spiral coils. The decision could be made according to various standards such as

(1) Distance itself
(2) Transfer loss
(3) Frequency tolerance of the source

These quantities somewhat contradict each other, and thus, there should be a judgement for the priority. In Fig. 13, measured coupling coefficient is shown as a function of the coil distance, where we choose the distance first, then the coupling coefficient k is decided. The measurement is carried out using a vector network analyzer. Two sets of spiral and loop coils as shown in Fig. 3 is faced each other, and S_{21} is measured that has two resonant peaks f_1, f_2 due to mutual coupling. The coupling coefficient k is calculated by the relation

$$k = \frac{f_2^2 - f_1^2}{f_2^2 + f_1^2} \tag{17}$$

Furthermore, from the relation

$$k = \frac{M}{\sqrt{L_1 L_2}} \tag{18}$$

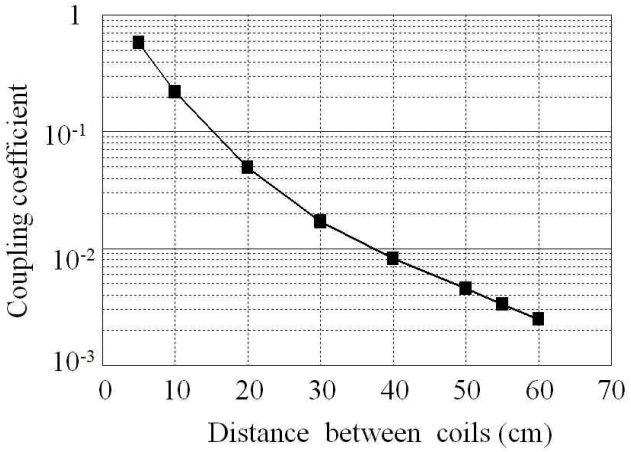

Fig. 13. Coupling coefficient of spiral coils (Pitch: 1 cm, Diameter: 25.5 cm, f_r: 25 MHz).

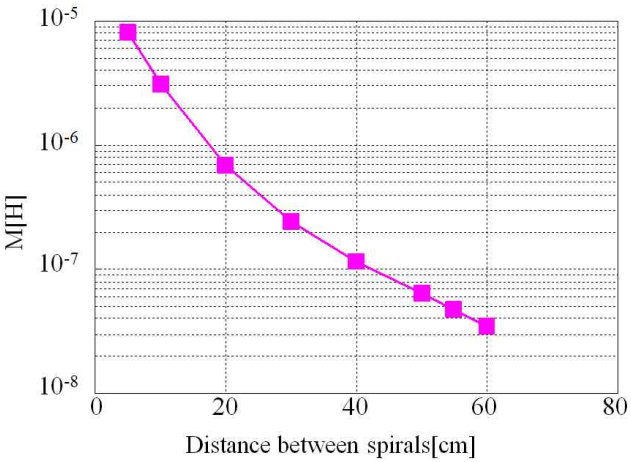

Fig. 14. Mutual inductance of spiral coils.

and Fig. 13, one can find the mutual inductance of two spiral coils as a function of the coil spacing as shown in Fig. 14.

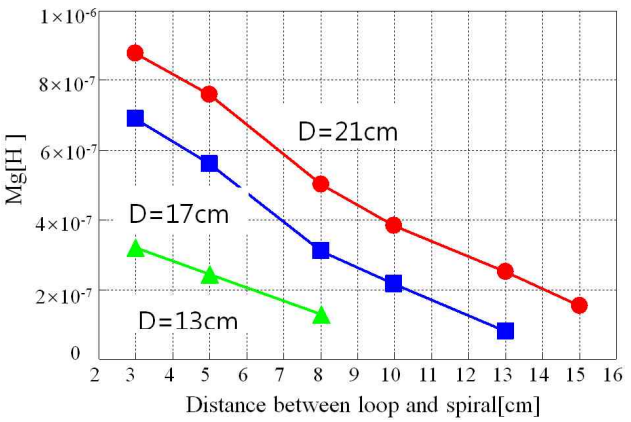

Fig. 15. Mutual inductance between loop and spiral coils (D is diameter of loop coil).

In the next, we will move on to the loop coil. The self inductance of loop coil is measured with an LC meter in the same way as the spiral coil. But the mutual inductance between a loop and spiral coils needs a small elaboration. For the circuit in Fig. 5, the input impedance Z_{in} is given as

$$Z_{in} = j\omega L_g \frac{1-(\omega/\omega_r)^2}{1-(\omega/\omega_a)^2} \tag{19}$$

where

$$\omega_r^2 = \frac{1}{LC\left(1-M_g^2/LL_g\right)} \tag{20}$$

$$\omega_a^2 = \frac{1}{LC} \tag{21}$$

Hence, M_g is calculated by the relation

$$M_g = \frac{1-(\omega_a/\omega_r)^2}{\sqrt{LL_g}} \tag{22}$$

since L and L_g are known, while ω_r and ω_a are measured from the input impedance for the structure shown in the inset of Fig. 3 using a VNA. The result is described in Fig. 15 for three different loop diameters. The mutual inductance increases as the loop diameter increases as long as it is less than that of the spiral coil.

Ⅵ. System Design and Measurement

We will design, simulate, construct and measure 2 systems with different distances between the spiral coils. Though the system with different source and load impedances is also quite important, we will not construct it this time, because the VNA with 50 Ω input impedance can not cope with the system with different impedance easily. Fig. 16 explains the experimental configuration.

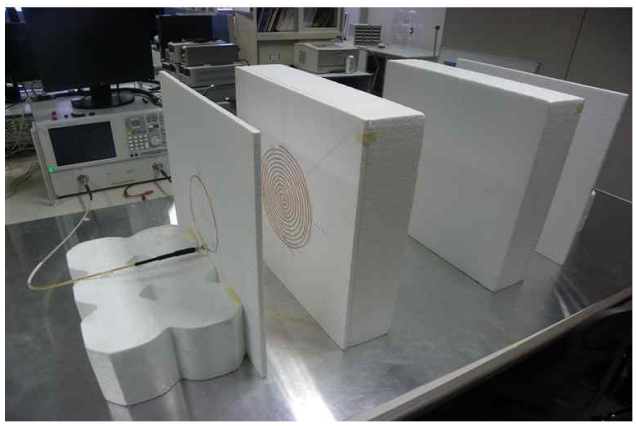

Fig. 16. Experimental setup.

We have chosen a spiral coil of 1 cm pitch. Winding it from the center, the diameter ended up with 25.5 cm to have the resonant frequency 25 MHz. The measured inductance L was 14.0 μH. Calculation with eq. (16) and measured inductance gives 2.90 pF for the effective capacitance C.

First example takes the distance between spiral coils as 30 cm, and then, the coupling coefficient is 0.017 consulting with Fig. 13. The mutual inductance M is known by Fig. 14 as 0.248 μH. Since the loop coil at the source side can be chosen freely, we wound a one-turn loop with the diameter 21 cm. The measured inductance is 0.80 μH. Though the loop coil at the load side should be determined by use of eq. (12), it is taken the same as that for the source side, because we are adopting the same impedance 50 Ω for the source and load.

The mutual inductance between the spiral and loop coils is to be calculated and the distance between both coils is to be obtained. The calculation is carried out by eqs. (10) and (11) to obtain 0.759 μH for both coils while it is used to obtain the distance 5.0 cm between the coils, consulting with Fig. 15. The results are summarized in Table 1 and Fig. 17.

All the values obtained above for the circuit elements are used for the circuit simulation, and give the frequency response shown in Fig. 18. The experimental result for the configuration in Fig. 17 is also shown in the same figure.

Table 1. Circuit parameters for designed system.

(a) Given parameters		(b) Calculated parameters	
f_r	2.50E+07 Hz	C	2.90E-12 H
R_g	50 Ω	M	2.48E-07 H
R_1	50 Ω	Q_{eg}	2.51
L	1.40E-05 H	M_g	7.59E-07 H
k	0.0177	k_g	0.227
L_g	8.00E-07 H	L_1	8.00E-07 H
		M_1	7.59E-07 H

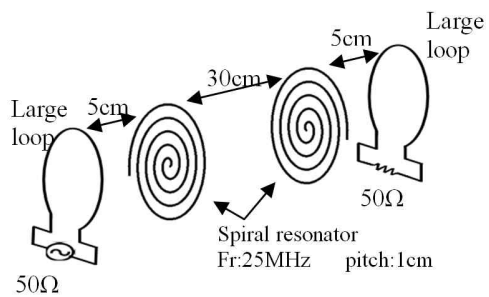

Fig. 17. Configuration of designed system.

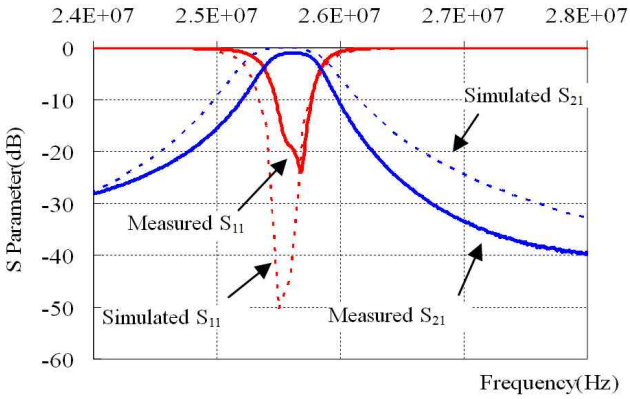

Fig. 18. Frequency characteristics of designed system.

There are two differences between the simulated and measured results. First, the measured bandwidth is about 2/3 of simulation. It is probably because the coupling between the spiral coils is not purely magnetic, but includes the electric component. The simulation that assumes purely magnetic coupling should overestimate the coupling coefficient, resulting in a larger bandwidth. Secondly, there is an attenuation pole for the measured result, which is not known why at this moment.

Another discrepancy of both results from the design is the shift of the center frequency from the designed value 25 MHz. It is because we did not adjust the frequency referring to eq. (13). We have not succeeded to shift the value of parasitic capacitance of a spiral coil effectively, and hence, we left the capacitance C as it is.

Table 2 and Fig. 19 show a design example for smaller coupling between spiral resonators. The simulated and measured results of constructed system are shown in Fig. 20, exhibiting a fairly good agreement with the designed value, again.

In spite of the deficiencies mentioned above, the simulated and measured values reasonably agree with the design. After small improvements, the theory will become more effective for resonator-coupled WPT systems.

Table 2. Circuit parameters for smaller coupling between spiral resonators.

(a) Given parameters		(b) Calculated parameters	
f_r	2.50E+07 Hz	C	2.902E-12 H
R_g	50 Ω	M	1.085E-07 H
R_1	50 Ω	Q_{eg}	2.510
L	1.40E-05 H	M_g	5.025E-07 H
k	0.0177	k_g	0.1501
L_g	8.00E-07 H	L_1	8.00E-07 H
		M_1	5.025E-07 H

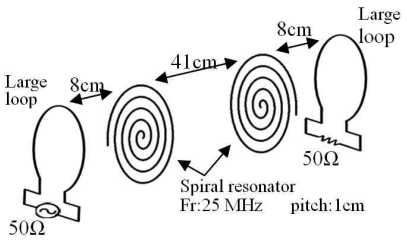

Fig. 19. Configuration for smaller coupling between spiral resonators.

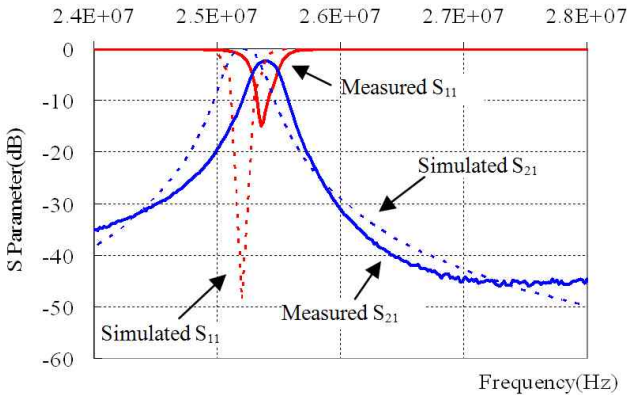

Fig. 20. Frequency characteristics for the configuration in Fig. 19 and Table 2.

VII. Conclusions

We have developed a design method of wireless power transfer systems based on magnetically coupled resonators, for the first time. It makes use of the filter design theory, considering the WPT system a bandpass filter. Unique modification of the filter theory has been carried out to cope with the WPT systems.

Design starts from obtaining the equivalent circuit of the WPT system. Parametric property of each circuit element obtained by EM simulation or measurement is used to realize the system, comparing it with the designed element values

Two design examples elucidate the feasibility of the proposed method. But further refinement of the method is required to attain exact agreement for the design and realized system response.

References

[1] A. Kurs, A. Karalis, R. Moffatt, J. D. Joannopoulos, P. Fisher, and M. Soljacic, "Wireless power transfer via strongly coupled magnetic resonances," *Science*, vol. 317, pp. 83-86, Jul. 2007.

[2] G. Matthaei, L. Young, and E. M. T. Jones, *Microwave Filters, Impedance-Matching Networks, and Coupling Structures*, Norwood, MA, Artech House, 1980.

[3] Ikuo Awai, Takuya Komori, "A simple and versatile design method of resonator-coupled wireless power transfer system," *Proc. 2010 International Conference on Communications, Circuits and Systems*, pp. 610-616, Jul. 2010.

[4] Ikuo Awai, "Design theory of wireless power transfer system based on magnetically coupled resonators," *Proc.2010 IEEE International Conference on Wireless Information Technology and Systems*, Aug. 2010.

Ikuo Awai

received the B.S. degree in 1963, M.S. degree in 1965, and Ph.D. in 1978, all from Kyoto University, Kyoto, Japan. In 1968, he joined Department of Electronics, Kyoto University, Japan, as a research associate, where he was engaged in the research on microwave magnetic waves and integrated optics. From 1984 to 1990, he worked for Uniden Corporation, Japan, developing microwave communication equipments. He joined Yamaguchi University as a professor in 1990, where he has studied magnetostatic wave devices, dielectric waveguide components, superconducting devices and artificial dielectrics for microwave application. In 2004, he started to work for Ryukoku University as a professor, being mainly engaged in microwave filters, metamaterials and wireless power transfer. He received the paper award from IEICE in 2002. He served as the chair of the Technical Group on Microwaves, IEICE, the chair of IEEE MTT-S Tokyo Chapter, Kansai Chapter and the chair of IEEE Hiroshima Section. Dr. Awai is a Fellow of IEICE and MTT society of IEEE.

Tetsuya Ishida

received the ME degrees from Ryukoku University Japan in 2007. In the same year, he joined Daihatsu Techner Co., Ltd. He is engaged in development of vehicle noise and vibration reduction. Additionally, he is engaged in R&D of microwave resonator and wireless power transmission, since he has belonged to a doctor's course of Ryukoku University in 2010.